International Journal of Naval Architecture and Ocean Engineering 12 (2020) 645–656

Contents lists available at ScienceDirect

International Journal of Naval Architecture and Ocean Engineering

journal homepage: http://www.journals.elsevier.com/international-journal-of-naval-architecture-and-ocean-engineering/

An advanced technique to predict time-dependent corrosion damage of onshore, offshore, nearshore and ship structures: Part II = Application to the ship's ballast tank

Do Kyun Kim [a, b], Hui Ling Lim [c], Nak-Kyun Cho [d, *]

[a] Marine Offshore and Subsea Technology Group, Newcastle University, NE1 7RU Newcastle upon Tyne, UK
[b] Graduate Institute of Ferrous Technology, POSTECH, 37673, Pohang, South Korea
[c] Ocean & Ship Technology (OST) Research Group, Universiti Teknologi PETRONAS, 32610, Seri Iskandar, Perak, Malaysia
[d] Department of Manufacturing Systems and Design Engineering, SeoulTech, 01811, Seoul, South Korea

ARTICLE INFO

Article history:
Received 17 March 2020
Received in revised form
11 May 2020
Accepted 1 July 2020
Available online 24 August 2020

Keywords:
Corrosion modelling
Time-dependent
Non-linear corrosion
Ballast tank
Pitting corrosion

ABSTRACT

In this study (Part II), the empirical formulation of corrosion model of a ship's ballast tank was developed to predict nonlinear time-dependent corrosion wastage based on the advanced data processing technique proposed by Part I. The detail on how to propose generalised mathematical formulation of corrosion model was precisely documented in the previous paper (Part I). The statistical scatter of corrosion data at any exposure time was investigated by the refined method and formulated based on a 2-parameter Weibull distribution which selected the best fit PDF. Throughout the nine (9) steps, empirical formulation of the ship's seawater ballast tank was successfully proposed and four (4) key step results were also obtained. The proposed method in Part I was verified and confirmed by this application of seawater ballast tank, thus making it possible to predict accurate behaviours of nonlinear time-dependent corrosion. Developed procedures and obtained corrosion damage model for ship's seawater ballast tank can be used for development of engineering software.

© 2020 Society of Naval Architects of Korea. Production and hosting by Elsevier B.V. This is an open access article under the CC BY-NC-ND license (http://creativecommons.org/licenses/by-nc-nd/4.0/).

1. Introduction

In general, the design life of infrastructures such as onshore, nearshore, offshore, and marine structures is considered as an important factor for both owner (=client) and builder (=constructor). In the case of marine structure, especially ship structure, the lifecycle starts with the conclusion of a contract including insurance matter, steel cutting, construction, operation, maintenance including regular and irregular inspection, repair by re-docking, and ends with the decommissioning (or demolition) process. All the processes should be made with proper decision-making. The ship-building market can be categorised by 1) the new-building market, freight market, sale and purchase (or second-hand) market, and decommissioning market. In general, this market is owned by ship owners based on the world cargo volume and market conditions including long and short economic-business cycles which are closely affecting the shipping cost and value of ship for the consideration of new-building, choice of used ship, and decision of decommissioning (Kim, 2010).

Over the last few decades, the investment of ship market has rapidly expanded to meet the high demand of the quantity of goods transported. In this regard, a number of efforts were made to extend the ship's economic life (=operation life or design life). In the early 21st century, Goal Based Standards (GBS) for new ship construction, which were proposed to enhance the functional requirement and ensure the safety goal during the design life of the ship, have been discussed and related regulations have been approved by IMO (2010). These regulations will be applied to tanker and bulk carrier with above 150m length ships starting construction from 1st July 2016. The specified design life of ship to determine the environmental condition and corrosive environment is defined as a principal design parameter. For example, 25 years of specific design life by considering Northsea environmental condition is applicable for oil tanker and bulk carrier specified in Tier II: functional requirement by the International Maritime Organisation (IMO, 2015) and the detail may be referred to in Fig. 1. It can be summarised that the GBS was proposed to construct safe and

* Corresponding author.
E-mail address: nkcho@seoultech.ac.kr (N.-K. Cho).
Peer review under responsibility of Society of Naval Architects of Korea.

https://doi.org/10.1016/j.ijnaoe.2020.07.002
2092-6782/© 2020 Society of Naval Architects of Korea. Production and hosting by Elsevier B.V. This is an open access article under the CC BY-NC-ND license (http://creativecommons.org/licenses/by-nc-nd/4.0/).

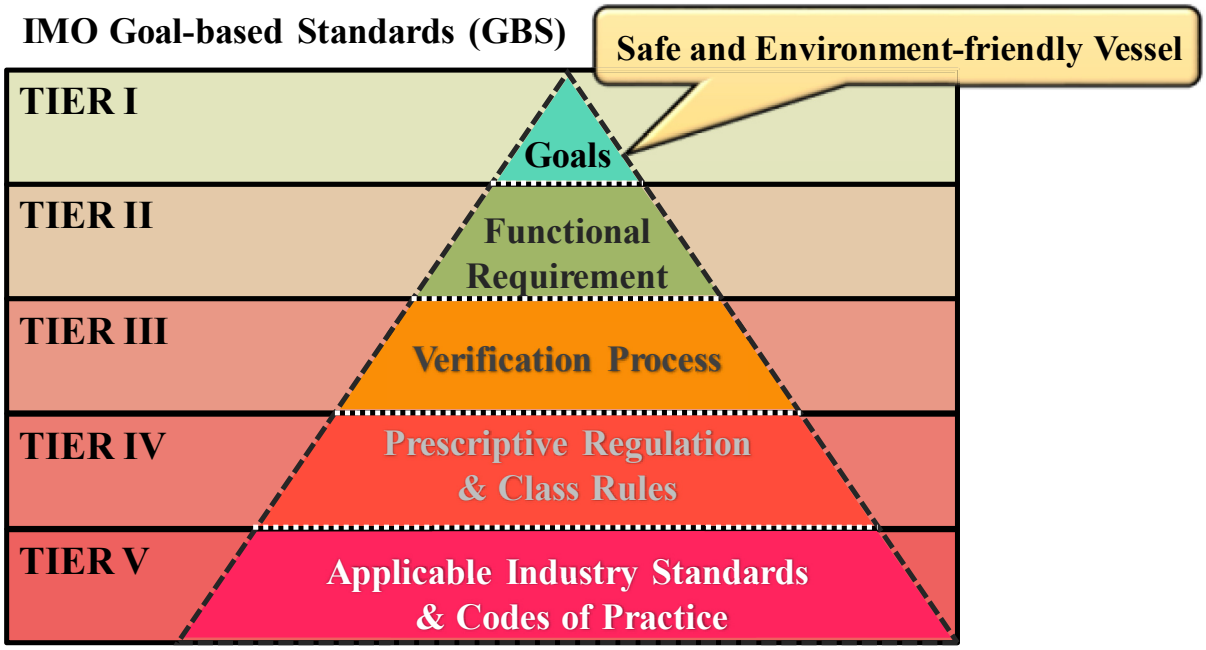

Fig. 1. Structure of goal-based standards by the international maritime organisation (IMO, 2015).

environmentally friendly structures by considering the intact and specified damage conditions throughout their life.

Among others, one of the important factors causing the degradation of ships and offshore structures is corrosion damage together with other issues such as fatigue cracking and localised dent. In general, this corrosion damage shows nonlinear behaviour with time which brings difficulties to predict the accurate amount of time-dependent corrosion wastage. A number of studies on the development of time-dependent corrosion wastage model to predict nonlinear behaviour of corrosion growth have been widely conducted by several researchers in two different ways using physical and plausible empirical models.

In the case of plausible physical model, Melchers and his research group (Melchers, 2001; Paik and Melchers, 2008) investigated and derived the basis of the physical corrosion progress. They have successfully developed their own corrosion model including a wide range of fundamental knowledge (Melchers, 2003a; b; 2012, Melchers et al., 2016; Petersen and Melchers, 2016). Chernov and his research team also studied physical corrosion models (Chernov 1990; Chernov and Ponomarenko, 1991). With regards to the empirical model, it is required to adopt probabilistic techniques with obtained corrosion wastage measurements. Guedes Soares and his research group proposed several corrosion damage models for ships and offshore structures (Guedes Soares and Garbatov, 1998; Guedes Soares et al., 2005, Guedes Soares et al., 2008; Garbatov et al., 2007; Garbatov and Guedes Soares, 2008, 2017; Kim et al., 2017). Paik and his group also widely investigated corrosion phenomenon and proposed several time-dependent corrosion wastage models such as oil tanker and FPSO (Paik et al., 2003), bulk carrier (Paik et al., 2003) and ballast tank (Paik et al., 2004) by adopting probabilistic approaches. In addition, Yamamoto and Ikegami (1998) investigated on corrosion wastage in the different components of ships.

Recently, Paik and Kim (2012) proposed an advanced technique to predict corrosion wastage by considering the formulation of sub-parameter of probability density function as a function of time applied to offshore well tube (Mohd Hairil and Paik, 2013) and subsea gas pipeline (Mohd Hairil et al., 2014). Recently, probabilistic data processing technique is proposed and applied in predicting current profile (Kim et al., 2019). In addition, refined regression analysis technique or artificial neural network (ANN) based data processing technique is also highlithed (Kim et al., 2019; Wong and Kim, 2018). A refined technique was most recently proposed together with the final outcome as a shape of empirical formulation (Kim et al., 2020). In the present study, a time-dependent corrosion wastage model for a ship's seawater ballast tank was developed by adopting the refined technique proposed in Part I (Kim et al., 2020). A number of application studies related to the structural safety assessment of corroded structures have widely been conducted based on existing time-dependent corrosion wastage models (Bai et al., 2016; Kim et al., 2012a, 2012b, 2014; Mohd Hairil et al., 2014; Rajput et al., 2019; Yang et al., 2016), corrosion margin based industrial corrosion practices (Kim et al., 2012, 2014, 2015; Paik et al., 2009), pitting corrosion (Rahbar-Ranji et al., 2015; Wang et al., 2018, 2020a, 2020b) and many others (Cui et al., 2019; Ozguc, 2020; Ringsberg et al., 2018). The proposed technique and corrosion model by the present study may help in predicting accurate residual strength of corroded structures.

2. Development of empirical formulation of time-dependent corrosion model of seawater ballast tank

From the previous study (Part I), the flowchart shown below in Fig. 2 has been proposed to formulate a generalised time-dependent corrosion wastage model. Based on the obtained procedure, a time-dependent corrosion wastage model of seawater ballast tank of aged ship was proposed with a total of 1935 corrosion measurements for ships aged 11–27 years (Paik et al., 2004).

2.1. Collection of corrosion data at various times (Step 1)

In the case of corrosion data, a total of 1,935 corrosion measurements of seawater ballast tank from the aged ships were used as shown in Fig. 3(a). However, details of the corrosion year

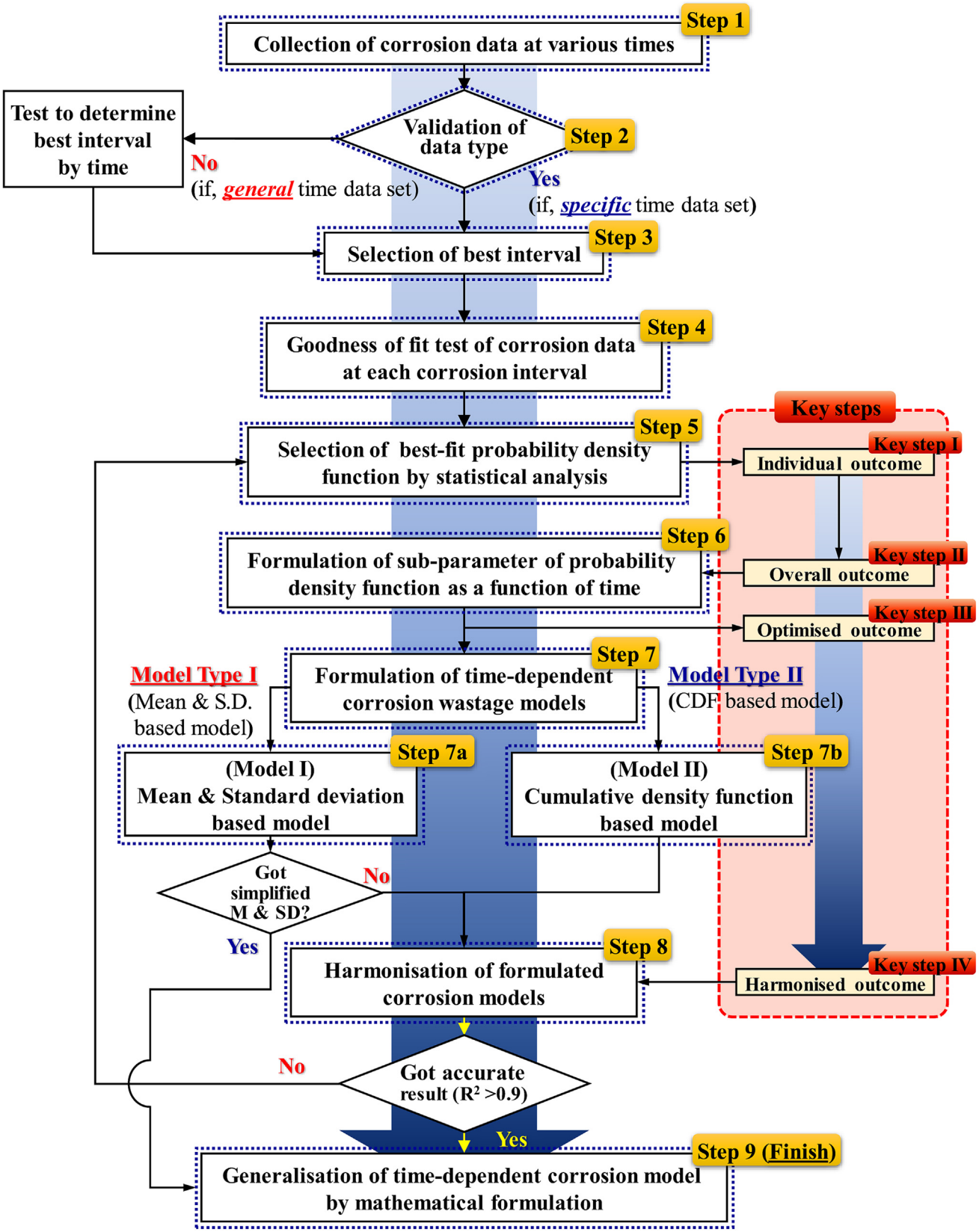

Fig. 2. Procedure to develop the time-dependent corrosion model by Part I (Kim et al., 2020).

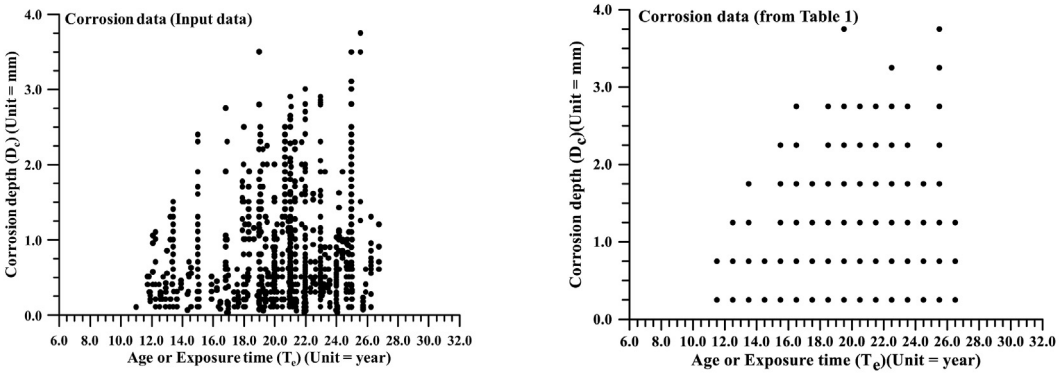

(a) Original corrosion data (Paik et al. 2004) (b) Input corrosion data (Present study)

Fig. 3. Collected pitting corrosion damage depth versus age of seawater ballast tank.

information were not provided from the previous study and only limited information of corrosion data was shared as illustrated in Table 1. Originally, corrosion measurements were opened based on the half-year (0.5 year) time interval and it was merged by the one-year (1 year) time interval in the present study as presented in Table 1 which was re-plotted in Fig. 3(b).

2.2. Validation of data type (Step 2)

Once corrosion data was collected in Step I, validation of data type was performed. If the detailed corrosion measurements could be achieved, they can then be considered as "General time data set"; however, the collected corrosion data of seawater ballast tank in the present study shown in Table 1 should be considered as "Specific time data set" with the one (1) year time interval.

2.3. Selection of the best interval (Step 3)

For the selection of the best interval, several methods have been introduced in Part I and all of those methods can be utilised if the corrosion data type was the general time data set. In the case of the present study, specific time data set of corrosion data was adopted so that this step can be skipped. One (1) year time interval was selected as the best interval from Table 1.

2.4. Goodness of fit test of corrosion data at each year (Step 4)

In the present study, the Anderson-Darling (A-D) test method was adopted for the goodness of fit test of the collected corrosion data based on probabilistic assessment. The A-D test result of each year was summarised in Table 2. From the previous step, one (1) year interval was selected as the best interval which as presented in Table 2. From the next step (Step 5), a detailed process to propose time-dependent corrosion wastage model of seawater ballast tank was documented with four (4) key steps.

2.5. Selection of the best-fit probability density function by statistical analysis (Step 5)

As highlighted in Part I, the lowest value obtained by the A-D test represented the best fit distribution. In Table 2, the best-fit distribution of each year was highlighted in bold. For example, 5.974 of Weibull distribution and 6.229 of Exponential distribution were selected as the best-fit probability density function (PDF) for 11–12 year and 12–13 year time range, respectively. In addition, the average value of each distribution was presented in the last column in Table 2 that showed Weibull distribution was finally selected as the best fit PDF with an average A-D value of 12.311.

2.5.1. - Individual outcome (Key step I)

Individual outcome was produced based on the selected

Table 1
Collected pitting corrosion data at various times (Paik et al., 2004).

Age (or exposure time) (Te, unit = years)	Pit depth or reduction of plate thickness (Dc, unit = mm)							
	0.0–0.5	0.5–10	1.0–1.5	1.5-2.0	2.0–2.5	2.5-3.0	3.0–3.5	3.5-4.0
11–12	20	5	0	0	0	0	0	0
12–13	29	5	9	0	0	0	0	0
13–14	25	28	30	2	0	0	0	0
14–15	4	5	0	0	0	0	0	0
15–16	31	14	10	3	2	0	0	0
16–17	17	8	5	2	1	1	0	0
17–18	103	2	2	4	0	0	0	0
18–19	35	26	39	9	4	3	0	0
19–20	137	20	12	8	9	2	0	1
20–21	179	62	22	13	17	2	0	0
21–22	114	116	28	26	7	6	0	0
22–23	52	57	5	12	7	5	3	0
23–24	75	49	12	5	3	5	0	0
24–25	59	42	10	2	0	0	0	0
25–26	40	50	49	59	40	2	2	3
26–27	8	15	2	0	0	0	0	0

Table 2
Results of goodness of fit test by Anderson-Darling (A-D) method.

Dist.	Age (Te, unit = yrs)															
	11–12	12–13	13–14	14–15	15–16	16–17	17–18	18–19	19–20	20–21	21–22	22–23	23–24	24–25	25–26	26–27	Ave.
Normal	6.526	7.545	5.926	1.488	5.392	2.952	37.067	5.167	35.155	39.134	22.297	13.174	15.478	11.868	6.099	3.009	13.674
Lognormal	6.526	7.690	8.108	1.488	6.098	3.047	37.563	8.443	35.489	37.983	22.192	9.528	14.411	14.345	14.036	3.699	14.417
3P- Lognormal	–	8.902	6.033	–	10.456	5.874	38.528	23.892	42.581	54.819	54.503	26.033	25.865	20.012	6.872	3.154	23.411
Exp.	6.168	6.229	9.728	1.624	5.032	2.499	35.606	8.752	29.836	31.178	22.490	9.156	12.957	13.782	20.875	4.390	13.756
2P-Exp.	32.692	45.220	19.638	1.888	36.304	14.334	346.946	27.707	376.477	434.033	156.546	54.485	117.672	91.755	27.539	5.299	111.878
Weibull	5.974	6.984	6.880	1.737	5.11	2.580	34.762	5.951	31.489	33.259	17.936	8.681	12.304	11.934	8.055	3.337	12.311
3P-Weibull	–	8.172	19.755	–	10.366	5.805	35.504	26.780	38.402	51.545	58.641	28.088	25.839	19.895	9.112	5.212	24.525
Smallest EV	5.974	7.071	5.536	1.737	5.785	3.545	34.890	6.965	34.779	41.996	29.359	16.257	20.185	11.627	8.521	2.817	14.935
Largest EV	7.985	8.903	6.531	1.610	6.249	3.180	44.358	6.118	40.647	42.167	21.046	10.803	15.030	14.610	7.763	3.406	15.036
Gamma	6.688	7.731	7.144	1.644	5.672	2.860	37.925	6.648	35.321	37.022	19.552	9.238	13.529	13.393	9.711	3.554	13.604
3P-Gamma	–	9.408	32.072	–	13.966	7.925	40.346	41.145	41.493	61.062	87.288	40.690	34.678	27.568	98.915	9.623	39.027
Logistic	6.664	7.258	5.685	1.462	5.157	2.718	37.624	5.122	33.974	35.796	19.881	11.394	13.229	11.861	6.480	3.120	12.977
Loglogistic	6.664	7.406	7.453	–	5.826	2.974	38.295	7.885	35.203	36.607	21.597	9.351	14.088	13.564	11.853	3.622	14.834
3P-Loglogistic	–	8.284	5.686	–	9.272	5.206	39.117	22.414	40.824	49.570	49.305	23.677	22.925	17.740	6.816	3.121	21.733

Note: Dist. = distribution, P = parameter, Exp. = exponential, EV = extreme value.

individual best fit distributions. For example, Table 3 shows the summarised best fit PDF types which were shortlisted from Table 2 by adopting the A-D test.

It was then possible to produce individual outcome (Key step I) based on selected individual best fit PDFs as illustrated in Table 3. Fig. 4 represents the plotting result based on Table 3. As expected, corrosion data of each year produced individually different types of probability density functions. Based on the obtained individual outcome, the blending processes such as Key step II to IV needed to be performed.

2.5.2. - Overall outcome (Key step II)

In the previous Key step I, individual outcome was achieved and 2-parameter Weibull distribution (herein Weibull PDF) consisted of scale and shape parameters was selected as the best fit PDF as shown in Eq. (1).

Selected best fit PDF: Weibull distribution

$$PDF_{(General)} = f(x) = \frac{B}{A}\left(\frac{x}{A}\right)^{B-1} \cdot \exp\left[-\left(\frac{x}{A}\right)^{B}\right]. \quad (1)$$

where, A = scale parameter, and B = shape parameter.

Based on the achievement from Key step I, selected Weibull PDF was to be commonly applied to all year's corrosion data as shown in Table 4. It was highlighted that this step of converting individual outcome to overall outcome should be one of the important parts to maintain the accuracy of the expected corrosion model. The next step (Key step III) was closely related to the expression of corrosion behaviour by a simplified formulation.

Based on the selected best-fit PDF, overall outcomes for all year were plotted in Fig. 5. From the obtained overall outcome, we can simply see the individual probabilistic trend of corrosion data by one (1) PDF as shown in Eq. (1). However, it did not show the general trend of all corrosion data. In this regard, the empirical formulation of sub-parameter by time of PDF will be investigated in the next section.

2.6. Formulation of sub-parameter of probability density function as a function of time (Step 6)

Once best fit PDF was commonly applied to each time of the corrosion data set, it might be able to bring the possibility for the formulation of the sub-parameters as a function of time, meaning that sub-parameters can now be blended as the simple function shapes as shown in Fig. 6. It is observed in Fig. 6(b) that the tendency of the gradient changes after 20 years of ship age which will affect $B(t_e)$. As would be expected that the operation life of the vessel designed by pre-CSR (common structural rule) was 20 years at that time. Mohd Hairil and Paik (2013) also conduct similar study in predicting time-dependent corrosion wastage of subsea oil well tube. They could obseve the tendency of the gradient changes after 15 years and conclude that the corrosion rate of the structure tends to speed up once it reaches 16 years of age. In addition, we cautiously predict that as corrosion sensing technology advances, corrosion information measured over 30 years can each have its own error.

2.6.1. - Optimised outcome (Key step III)

From the data processing in the previous important steps, the probability behaviour of corrosion wastage by time can be expressed by a simple equation from Eq. (1) and Fig. 5, herein "Optimised outcome", as shown in Eq. (2).

$$PDF_{(present\ study)} = f\left(D_c\right)$$

Table 3
Details on individual outcome.

Age (= exposure time, yrs)	Information of selected best fit probability density distribution (PDF)				
	A-D value	Type of PDF	Sub-parameters		
			A	B	C
11–12	5.974	Weibull	0.3987	1.9217	–
12–13	6.229	Exponential	0.5174	–	–
13–14	5.536	SEV*	0.3957	–	1.0155
14–15	1.462	Logistic	0.1599	–	0.5401
15–16	5.032	Exponential	0.6750	–	–
16–17	2.499	Exponential	0.7353	–	–
17–18	34.762	Weibull	0.3705	1.4028	–
18–19	5.122	Logistic	0.3513	–	0.9125
19–20	29.836	Exponential	0.5701	–	–
20–21	31.178	Exponential	0.6280	–	–
21–22	17.936	Weibull	0.8515	1.4201	–
22–23	8.681	Weibull	0.9417	1.2701	–
23–24	12.304	Weibull	0.7303	1.2827	–
24–25	11.627	SEV*	0.4346	–	0.7471
25–26	6.099	Normal	0.7494	–	1.3276
26–27	2.817	SEV*	0.2936	–	0.7773
Average	11.693	Weibull	N/A		

Note: A, B, C for Weibull PDF are scale, shape and location parameter, in respectively. Details may be referred to Appendix A, Te = age or exposure time, SEV* = Smallest Extreme Value.

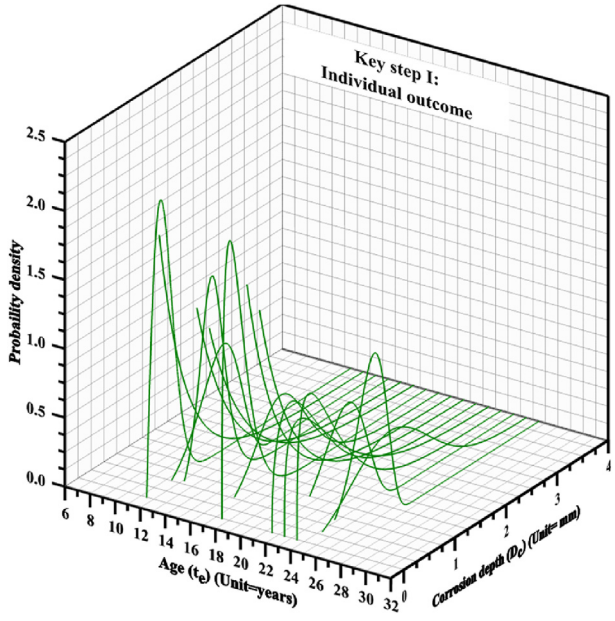

Fig. 4. The obtained individual outcome (Key step I).

$$= \frac{B(t_e)}{A(t_e)}\left(\frac{D_c}{A(t_e)}\right)^{B(t_e)-1} \cdot \exp\left[-\left(\frac{D_c}{A(t_e)}\right)^{B(t_e)}\right] \quad (2)$$

where, PDF = probability density function, D_c = corrosion depth, $A(t_e)$ = scale parameter by exposure time = $0.0004t_e^3 - 0.0248t_e^2 + 0.4796t_e - 2.3831$, and $B(t_e)$ = shape parameter by exposure time = $0.0020t_e^3 - 0.0995t_e^2 + 1.5618t_e - 6.0115$, t_e = exposure time.

As mentioned in Part I (Kim et al., 2020), sub-parameters such as $A(t_e)$ and $B(t_e)$ were formulated as a function of time by the curve fitting method shown in Fig. 6. Therefore, the optimised outcome was then obtained as shown in Fig. 7. As expected, the obtained outcome of "optimised outcome" was much more blended as compared with "overall outcome". In order to get accurate

Table 4
Details on overall outcome.

Age (= exposure time, yrs)	Information of selected best fit probability density distribution (PDF)				
	A-D value	Type of PDF	Sub-parameters		
			A	B	C
11–12	5.974	Weibull	0.3987	1.9217	–
12–13	6.984	Weibull	0.5739	1.3935	–
13–14	6.880	Weibull	0.9064	1.9650	–
14–15	1.737	Weibull	0.5988	2.3498	–
15–16	5.110	Weibull	0.7420	1.3474	–
16–17	2.580	Weibull	0.7972	1.2595	–
17–18	34.762	Weibull	0.3705	1.4028	–
18–19	5.951	Weibull	1.0584	1.5785	–
19–20	31.489	Weibull	0.5966	1.1043	–
20–21	33.259	Weibull	0.6745	1.2024	–
21–22	17.936	Weibull	0.8515	1.4201	–
22–23	8.681	Weibull	0.9417	1.2701	–
23–24	12.304	Weibull	0.7303	1.2827	–
24–25	11.934	Weibull	0.6210	1.6414	–
25–26	8.055	Weibull	1.4894	1.8038	–
26–27	3.337	Weibull	0.7122	2.3221	–

Note: A, B, C for Weibull PDF are scale, shape and location parameter, in respectively. Details may be referred to Appendix A. In the case of C, it represents location parameter which is applicable only for 3-parameter Weibull PDF.

"optimised outcome", it should be highlighted again that the step of empirical formulation by curve fitting in Fig. 6 should have higher R2 value, meaning that the obtained curves needed to be well-fitted with the original data.

2.7. Formulation of TDCWMs (Step 7)

Once the sub-parameters were defined, we can then develop two types of time-dependent corrosion wastage models (TDCWMs) such as 1) Mean & Standard Deviation based model and 2) Cumulative density function based model. Harmonisation process will be discussed in the coming section.

2.7.1. Model I: Mean & Standard Deviation based model (step 7a)

From the optimised outcome as shown in Eq. (2), mean and standard deviation values of Weibull distribution were obtained as

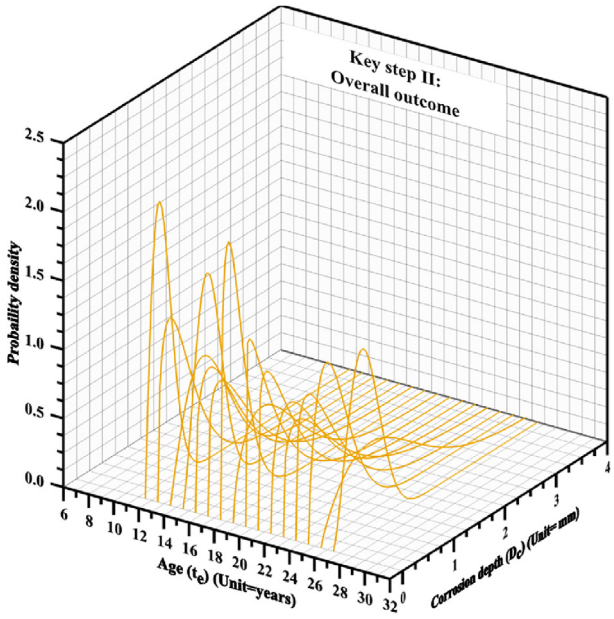

Fig. 5. The obtained overall outcome (Key step II).

shown in Eqs. (3.1) and (3.2).

$$M = A\left(t_e\right) \cdot \Gamma\left(1+\frac{1}{B(t_e)}\right) \tag{3.1}$$

$$SD = \sqrt{[A(t_e)]^2 \cdot \left[\Gamma\left(1+\frac{2}{B(t_e)}\right) - \Gamma^2\left(1+\frac{1}{B(t_e)}\right)\right]} \tag{3.2}$$

where, M = mean, SD = standard deviation, $A(t_e)$ = scale parameter by exposure time = $0.0004t_e^3 - 0.0248t_e^2 + 0.4793t_e - 2.3812$, and $B(t_e)$ = shape parameter by exposure time = $0.002t_e^3 - 0.0994t_e^2 + 1.5604t_e - 6.0025$.

Therefore, mean and standard deviation based model (Model I) can be proposed as shown in Eq. (4) based on five (5) different corrosion levels such as slight level (M - SD), average level (M), severe level I (M + SD), severe level II (M + 2SD), and severe level III (M + 3SD) as proposed in Part I.

2.7.2. Model II: cumulative density function based model (step 7b)

As noted in Part I, the above-mentioned corrosion model (Model I) for ship's seawater ballast tank consisted of Gamma function which may cause the inability to obtain the corrosion depth by direct hand calculation, meaning that another corrosion model (herein, Model II) based on cumulative density function (CDF) needed to be developed. In order to derive a CDF based corrosion model (Model II) shown in Eq. (5.1), it can be started from the integration of PDF as illustrated in Eq. (2). Once we integrated PDF by corrosion depth (D_c), CDF can be obtained as shown in Eq. (5.2).

Proposed Corrosion Model (Model I)

$$D_c = \begin{cases} M - SD & \textit{for Slight level} \\ M & \textit{for Average level} \\ M + SD & \textit{for Severe level I} \\ M + 2SD & \textit{for Severe level II} \\ M + 3SD & \textit{for Severe level III} \end{cases} \tag{4}$$

where, D_c = corrosion depth, M = mean value in Eq. (3.1), SD = standard deviation in Eq. (3.2).

Cumulative Density Function (CDF) of Weibull distribution

$$CDF_{(General)} = F(x) = \int PDF\, dx = \int f(x)\, dx = 1 - \exp\left[-\left(\frac{x}{A}\right)^B\right] \tag{5.1}$$

$$CDF_{(present\ study)} = F(D_c) = \int PDF\, dD_c = \int f(D_c)\, dD_c = 1 - \exp\left[-\left(\frac{D_c}{A(t_e)}\right)^{B(t_e)}\right] \tag{5.2}$$

From the obtained relationship between CDF and corrosion depth (D_c) in Eq. (5.2), Cumulative Density Function (CDF) based model can be summarised as Eq. (5.3).

Proposed Corrosion Model (Model II)

$$D_c = A(t_e) \cdot [-\ln(1 - CDF)]^{\left\langle \frac{1}{B(t_e)} \right\rangle} \tag{5.3}$$

where, D_c = corrosion depth; $A(t_e)$ = scale parameter by exposure time; $B(t_e)$ = shape parameter by exposure time.

As shown in Eq. (5.3), the proposed corrosion model II is the function of sub-parameters, i.e., $A(t_e)$ and $B(t_e)$, and CDF value. In the case of sub-parameters, those were defined as the shape of empirical formulation in Fig. 5. The effect of CDF value was investigated in Fig. 7. In general, 95% or above the value of probability

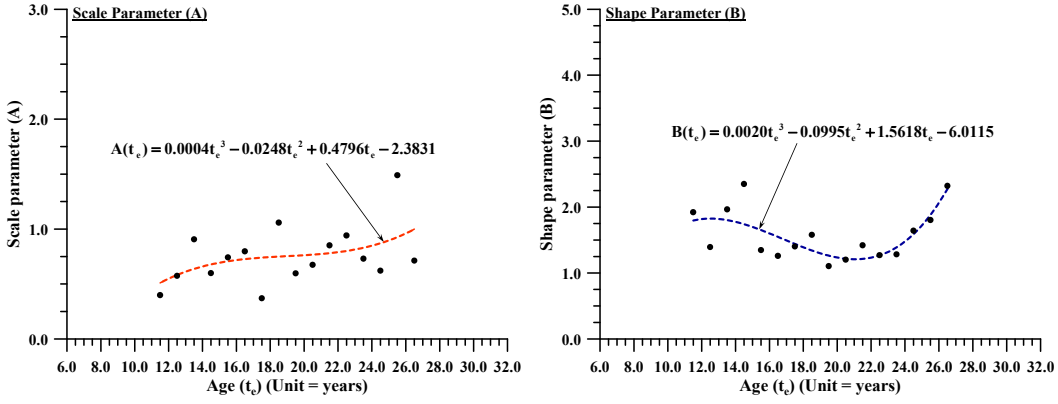

(a) scale parameter (b) shape parameter

Fig. 6. Empirical formulation of sub-parameter of probability density function as a function of time by curve fitting.

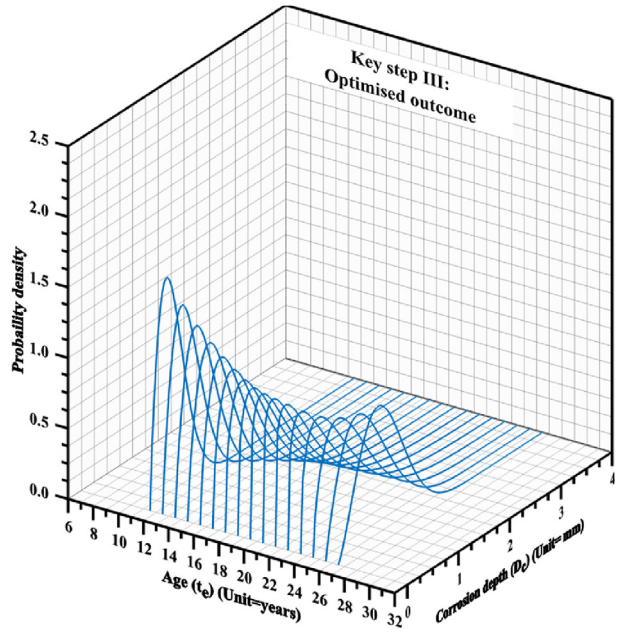

Fig. 7. The optimised outcome (Key step III).

density was applied for the design of structures and can be considered by 0.95 of CDF value in the present corrosion model.

For the research purpose, CDF values were increased at regular intervals of 0.05 from 0.05 to 0.95 as shown in Fig. 8. In addition, the starting time of the corrosion which is one of the important outcomes has been obtained by corrosion model as shown in Fig. 8. It was found that the starting time of the corrosion was independent from the CDF values which meant that only one (1) value of starting of corrosion time can be achieved by Eq. (5.3). In this ballast tank corrosion case, we can predict that it occurred after 7.585 years as shown in Fig. 8 by the proposed Eqns. (3.2) and (5.3). This can be done by extrapolation of $A(t_e)$ and $B(t_e)$ presented in Eq. (3.2).

However, some of the probability density functions (PDFs) with different types of corrosion data were made sure to not be able to predict the starting time of the corrosion as shown in a previous example (Part I). In this case, it was suggested to adopt the 2nd or 3rd best PDF to predict the starting time of the corrosion. Based on the obtained corrosion model II, harmonisation with Model I will be processed. In corrosion model I, corrosion models have been classified by five (5) levels based on their severity such as slight, average, and three severe levels. From the harmonisation process, the CDF value in corrosion model II will be decided based on five (5) corrosion levels.

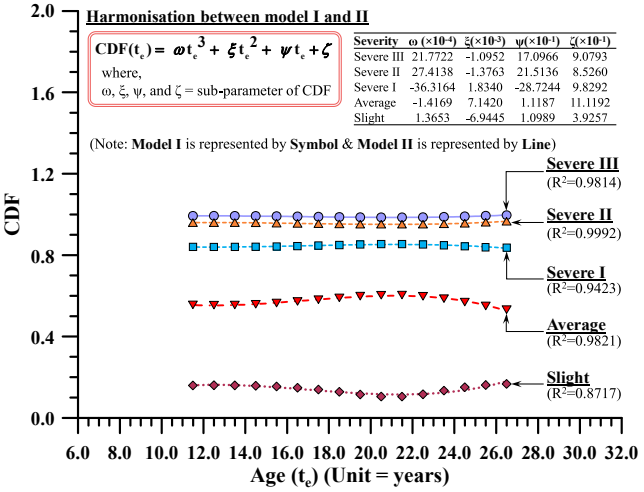

Fig. 9. Relationship between CDF and time.

Table 5
Sub-parameter of CDF.

$$CDF(t_e) = \omega\, t_e^{3} + \xi\, t_e^{2} + \psi\, t_e + \zeta \quad (7)$$

Severity	ω (× 10-4)	ξ(× 10-3)	ψ(× 10-1)	ζ(× 10-1)
Severe III	21.7722	−1.0952	17.0966	9.0793
Severe II	27.4138	−1.3763	21.5136	8.5260
Severe I	−36.3164	1.8340	−28.7244	9.8292
Average	−1.4169	7.1420	1.1187	11.1192
Slight	1.3653	−6.9445	1.0989	3.9257

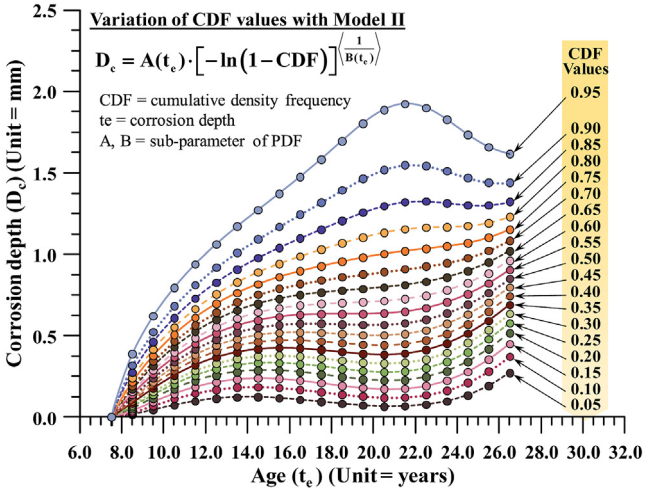

Fig. 8. Example of applied corrosion model with different CDF values.

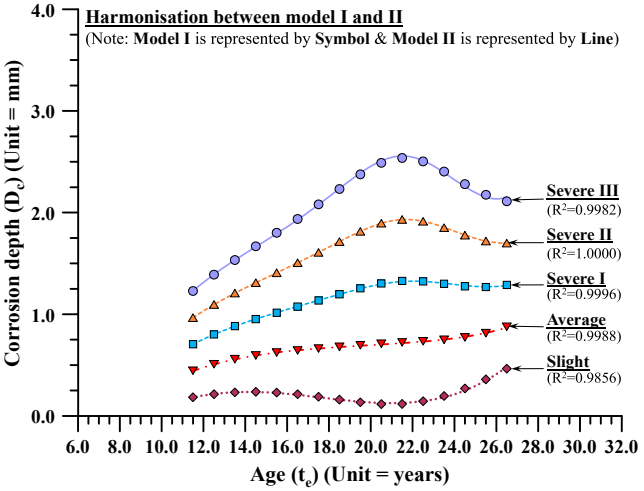

Fig. 10. The obtained harmonised outcomes for five corrosion levels (Key step IV).

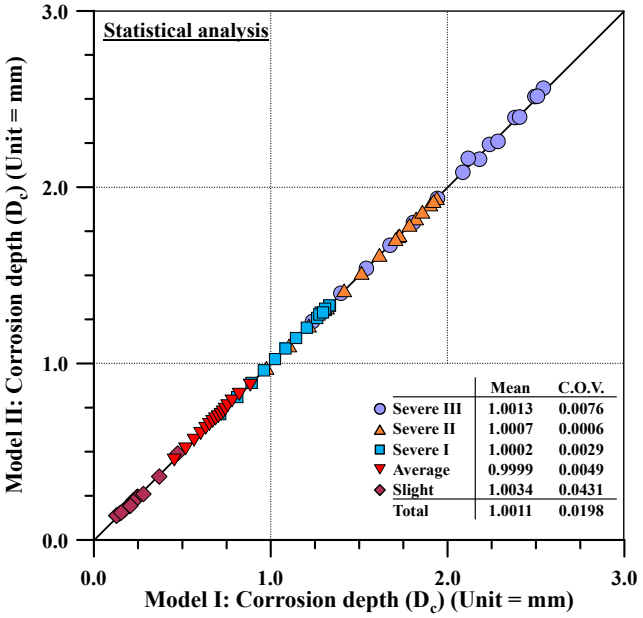

Fig. 11. Statistical analysis of obtained corrosion models.

2.8. Harmonisation of formulated corrosion models (Step 8)

2.8.1. - Harmonised outcome (Key step IV)

In this step, two proposed models, i.e., model I and II obtained in the previous section, will be compared to propose the harmonised outcome. Basically, harmonisation process started from the assumption that model I and II will produce similar results as shown in Eq. (6). For the reader's information, corrosion models I and II are presented in Eqs. (4) and (5.3), respectively.

$$Model\ I \simeq Model\ II \tag{6}$$

From the previous step, sub-parameters of PDF were defined and can be presented as a function of time. Here, we found that the CDF value was also affected by time. In this regard, CDF values are presented as function of time as shown in Fig. 9 and Eq. (7).where, ω ξ ψ, and ζ = sub-parameter of CDF which can be referred to Table 5.

From the assumption of Eq. (6), CDF values for five corrosion levels such as slight, average, severe I, severe II, and severe III can be achieved by investigation as shown in Fig. 10. In the harmonisation process, it was suggested that at least 0.9 or above 0.9 of coefficient of determination (R^2) values should be achieved for the harmonisation between Models I and II. In this study, 0.9856, 0.9856, 0.9996, 1.000, and 0.9982 of R^2 values were obtained from slight to severe III corrosion models as shown in Fig. 10.

In order to confirm the applicability of harmonised outcome, statistical analysis was additionally conducted in Fig. 11. From the mean and coefficient of variation (COV) values, it can be concluded that those two models, Models I and II have been harmonised very well and showed good agreement with each other. The details of statistical analysis result can also be referred to in Table 6.

2.9. Generalisation of time-dependent corrosion model by mathematical formulation (Step 9)

From the previous step 8, harmonisation between Models I and II was conducted and verified by the Coefficient of determination (R^2), Mean and COV values as illustrated in Fig. 10. If the R^2 value was above 0.9, it can then go through the generalisation step for the mathematical formulation of time-dependent corrosion model. If the R^2value did not satisfy the criterion (R^2= 0.9), it can then go back to Step 5 and the 2nd best PDF can be selected as the best-fit PDF.

As mentioned earlier in the whole procedure shown in Fig. 2, to develop a time-dependent corrosion wastage model, a total of four (4) key steps were highlighted: individual, overall, optimised and harmonised outcome and obtained outcomes as shown in Fig. 12(a)–12(d). Each outcome has been re-plotted as a shape of mean and standard deviation information together with the measured corrosion data of the ship ballast tank which is presented with a grey colour circle in Fig. 12. As would be expected, the mean value of corrosion data was blended step by step and finally, a very smooth curve shape of the corrosion model was obtained as shown in key step IV in Fig. 12(d).

The obtained outcomes of the average level of corrosion model by four (4) key steps were statically analysed again based on

Table 6
Data of statistical analysis for harmonisation.

Age (Years)	Slight			Average			Severe I			Severe II			Severe III		
	I	II	II/I	I	II	II/I	I	II	II/I	I	II	II/I	I	II	II/I
11–12	0.1926	0.1932	1.0029	0.4538	0.4533	0.9990	0.7149	0.7146	0.9995	0.9760	0.9764	1.0003	1.2372	1.2402	1.0024
12–13	0.2238	0.2255	1.0077	0.5174	0.5168	0.9989	0.8110	0.8105	0.9994	1.1046	1.1046	1.0001	1.3981	1.4009	1.0020
13–14	0.2415	0.2425	1.0045	0.5666	0.5665	0.9998	0.8917	0.8917	1.0000	1.2169	1.2169	1.0000	1.5420	1.5422	1.0001
14–15	0.2463	0.2451	0.9952	0.6039	0.6047	1.0014	0.9615	0.9624	1.0009	1.3190	1.3194	1.0002	1.6766	1.6731	0.9979
15–16	0.2395	0.2354	0.9829	0.6319	0.6337	1.0029	1.0243	1.0263	1.0019	1.4167	1.4176	1.0006	1.8091	1.8028	0.9965
16–17	0.2228	0.2168	0.9726	0.6535	0.6558	1.0035	1.0841	1.0868	1.0024	1.5147	1.5164	1.0011	1.9454	1.9392	0.9969
17–18	0.1987	0.1932	0.9724	0.6713	0.6730	1.0024	1.1440	1.1463	1.0020	1.6167	1.6190	1.0014	2.0893	2.0874	0.9991
18–19	0.1704	0.1692	0.9929	0.6877	0.6872	0.9993	1.2049	1.2051	1.0002	1.7222	1.7245	1.0013	2.2395	2.2454	1.0026
19–20	0.1435	0.1494	1.0409	0.7036	0.7001	0.9950	1.2637	1.2605	0.9975	1.8238	1.8250	1.0007	2.3839	2.3988	1.0063
20–21	0.1259	0.1378	1.0943	0.7187	0.7127	0.9917	1.3114	1.3053	0.9953	1.9042	1.9042	1.0000	2.4969	2.5179	1.0084
21–22	0.1271	0.1383	1.0886	0.7317	0.7261	0.9924	1.3362	1.3306	0.9958	1.9408	1.9409	1.0000	2.5454	2.5650	1.0077
22–23	0.1536	0.1552	1.0105	0.7430	0.7416	0.9981	1.3324	1.3316	0.9994	1.9218	1.9237	1.0010	2.5112	2.5195	1.0033
23–24	0.2057	0.1939	0.9426	0.7571	0.7614	1.0058	1.3084	1.3137	1.0040	1.8598	1.8632	1.0019	2.4111	2.4014	0.9960
24–25	0.2789	0.2605	0.9342	0.7812	0.7887	1.0096	1.2835	1.2912	1.0060	1.7859	1.7884	1.0014	2.2882	2.2630	0.9890
25–26	0.3686	0.3594	0.9750	0.8223	0.8268	1.0054	1.2760	1.2801	1.0032	1.7297	1.7299	1.0001	2.1834	2.1617	0.9901
26–27	0.4736	0.4914	1.0376	0.8850	0.8787	0.9929	1.2964	1.2915	0.9962	1.7078	1.7080	1.0002	2.1192	2.1665	1.0223
R^2	N/A		0.9856	N/A		0.9988	N/A		0.9996	N/A		1.0000	N/A		0.9982
Mean			1.0034			0.9999			1.0002			1.0007			1.0013
COV			0.0431			0.0049			0.0029			0.0006			0.0076

Note: I = Model I, II = Model II.

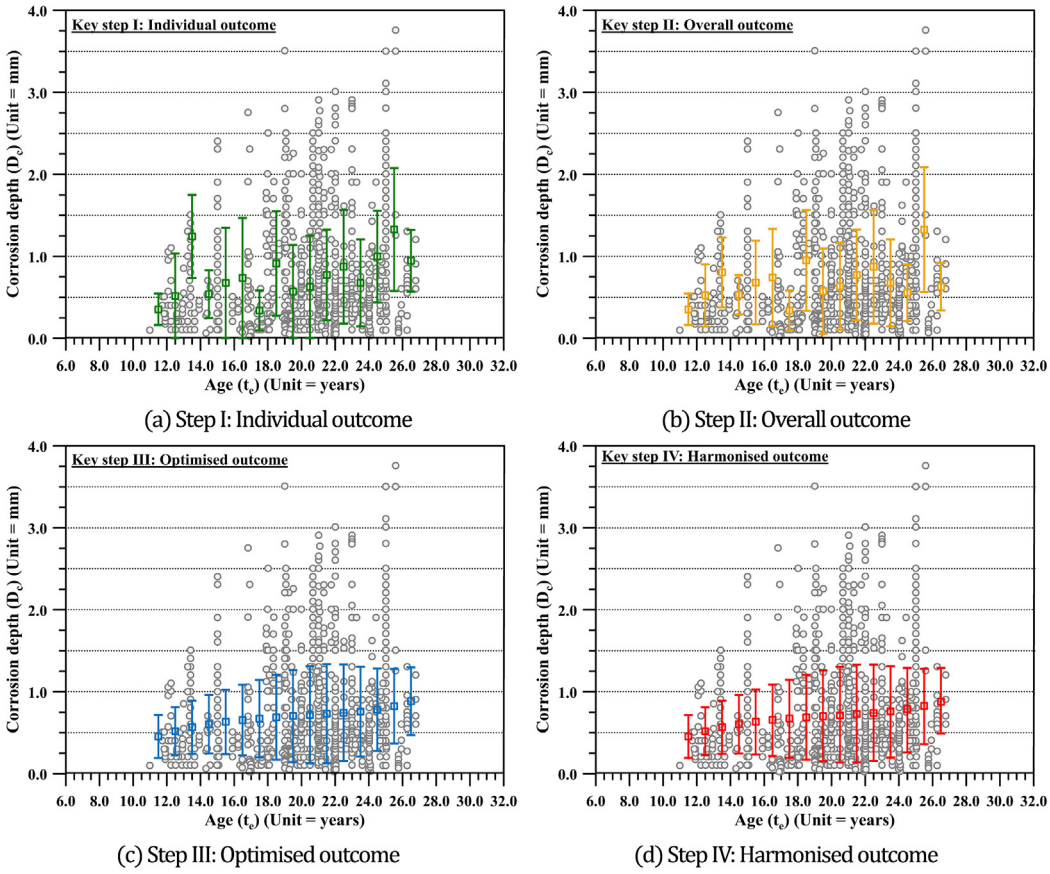

Fig. 12. The obtained key step results for ship ballast tank.

individual outcome which was set on a horizontal axis and others were put on a vertical axis in Fig. 13. The details can be referred to in Table 7. From the results in Fig. 13, individual and overall outcomes showed that corrosion damage was fluctuating as time goes by. The blended results were obtained once the optimisation step was done. After that, harmonised outcome, which was close to optimised outcome, can be obtained from the comparison between corrosion Models I and II. Once again, the harmonised outcome was based on corrosion Model II and it can help engineers to predict the accurate amount of corrosion damage in simple ways.

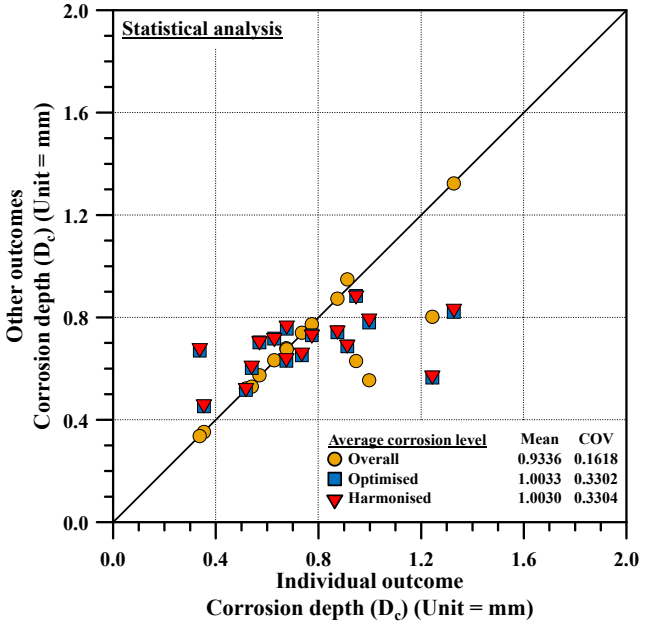

Fig. 13. Statistical analysis of the obtained average corrosion models.

Finally, the generalised shape of corrosion model shown in Eq. (8) can be proposed to predict time-dependent corrosion wastage of the ship's ballast tank with five different levels of corrosion such as slight, average, severe I, II and III.

Time-dependent corrosion model of ship's ballast tank

$$D_c = A(t_e) \cdot [-\ln(1 - CDF(t_e))]^{\left\langle \frac{1}{B(t_e)} \right\rangle} \quad \text{Eq. (8)}$$

where, D_c = time-dependent corrosion depth (mm), $A(t_e)$ = scale parameter by exposure time = $0.0004t_e^3 - 0.0248t_e^2 + 0.4793t_e - 2.3812$, $B(t_e)$ = shape parameter by exposure time = $0.002t_e^3 - 0.0994t_e^2 + 1.5604t_e - 6.0025$, and $CDF(t_e)$ = cumulative density function value which can be referred to in Eq. (7) and Fig. 9.

3. Concluding remarks

In the present study, the applicability of the proposed method to predict time-dependent corrosion wastage by Part I (Kim et al., 2020) was verified by corrosion data of a ship's ballast tank. As stated in the abstract part, three (3) objectives which are 1) starting of corrosion time, 2) remaining of corrosion life (if there are criteria of design life or minimum thickness requirement), and 3) corrosion

Table 7
Data of statistical analysis for key steps.

Age (Years)	Average level of corrosion						
	Individual	Overall	Optimised	Harmonised	Individual /Overall	Individual /Optimised	Individual /Harmonised
11–12	0.3536	0.3536	0.4538	0.4533	1.0000	1.2832	1.2819
12–13	0.5174	0.5234	0.5174	0.5168	1.0116	0.9999	0.9988
13–14	1.2438	0.8035	0.5666	0.5665	0.6460	0.4555	0.4554
14–15	0.5401	0.5306	0.6039	0.6047	0.9824	1.1180	1.1195
15–16	0.6750	0.6807	0.6319	0.6337	1.0084	0.9361	0.9388
16–17	0.7353	0.7412	0.6535	0.6558	1.0081	0.8887	0.8918
17–18	0.3376	0.3376	0.6713	0.6730	1.0000	1.9885	1.9933
18–19	0.9125	0.9501	0.6877	0.6872	1.0412	0.7536	0.7531
19–20	0.5701	0.5749	0.7036	0.7001	1.0085	1.2341	1.2279
20–21	0.6280	0.6342	0.7187	0.7127	1.0099	1.1444	1.1349
21–22	0.7744	0.7744	0.7317	0.7261	1.0000	0.9448	0.9376
22–23	0.8740	0.8740	0.7430	0.7416	1.0000	0.8502	0.8486
23–24	0.6764	0.6764	0.7571	0.7614	1.0000	1.1193	1.1258
24–25	0.9979	0.5555	0.7812	0.7887	0.5567	0.7828	0.7903
25–26	1.3276	1.3244	0.8223	0.8268	0.9976	0.6194	0.6228
26–27	0.9468	0.6310	0.8850	0.8787	0.6665	0.9347	0.9281
Mean					1.1112	1.1041	1.0030
Standard deviation (SD)					0.2487	0.3747	0.3314
Coefficient of variation (COV)					0.2238	0.3394	0.3304

wastage over time, were covered and time-dependent corrosion wastage could be predicted by the proposed corrosion model in the present study.

The obtained outcomes from the present study can be summarised as follows:

- The proposed method by Part I was verified by the corrosion data of a ship's ballast tank.
- Simple, accurate, and user friendly corrosion models for ship's ballast tank were developed which included five (5) corrosion levels such as slight, average, severe I, II, and III.
- In the case of the ship's ballast tank structure, the corrosion behaviour can be predicted by a 2-parameter Weibull probability density function (PDF).
- It was found that the corrosion of the ship's ballast tank occurred after 7.5 years of operation.

The limitations of the proposed time-dependent corrosion wastage model of the ship's ballast tank are also summarised as follows:

- As would be expected, the wrong data input will produce the wrong output, meaning that corrosion data should be measured accurately and new technologies on sensor should be focused on.
- In this ship's ballast wall corrosion model, it was recommended to use an average corrosion model. If the readers want to use other corrosion models such as slight, severe I, II, and III, it is recommended to use the models until 21 years which is the peak point of corrosion damage as shown in Fig. 10.
- For the development of corrosion model, some of the PDFs, i.e., normal, lognormal, 3-P lognormal, Gamma, 3-P Gamma, did not provide corrosion models as presented (which may referred to Table A2 provided by linin part I).

Finally, the advantages of a new technique to the proposed method proposed in Part I were confirmed by the present example study. However, it is recommended that further studies on different types of structure with corrosion data should be conducted and validated. The developed corrosion model for a ship's ballast tank will be very useful information to ship structural designers to predict time-dependent corrosion wastage which can also directly be used for wall thickness design. In addition, software development work based on obtained outcome will be further performed in the near future.

Acknowledgements

This research was supported by the Technology Innovation Program (Grant No.: 10053121 and 10051279) funded by the Ministry of Trade, Industry & Energy (MI, Korea). The authors would also like to thank SeoulTech, POSTECH, and Universiti Teknologi PETRONAS for their kind supports.

References

Bai, Y., Yan, H.B., Cao, Y., et al., 2016. Time-dependent reliability assessment of offshore jacket platforms. Ships Offshore Struct. 11 (6), 591–602.
Chernov, B.B., 1990. Predicting the corrosion of steels in seawater from its physiochemical characteristics. Protect. Met. 26 (2), 238–241.
Chernov, B.B., Ponomarenko, S.A., 1991. Physiochemical modelling of metal corrosion in seawater. Protect. Met. 27 (5), 612–615.
Cui, J., Wang, D., Ma, N., 2019. Case studies on the probabilistic characteristics of ultimate strength of stiffened panels with uniform and non-uniform localized corrosion subjected to uniaxial and biaxial thrust. Int. J. Naval Archit. Ocean Eng. 11 (1), 97–118.
Garbatov, Y., Guedes Soares, C., 2008. Corrosion wastage modeling of deteriorated ship structures. Int. Shipbuild. Prog. 55, 109–125.
Garbatov, Y., Guedes Soares, C., 2017. Spatial corrosion wastage modelling of steel plates subjected to marine environments. In: The 36th International Conference on Ocean, Offshore and Arctic Engineering (OMAE 2017), 25-30 June, Trondheim, Norway.
Garbatov, Y., Guedes Soares, C., Wang, G., 2007. Non-linear time dependent corrosion wastage of deck plates of ballast and cargo tanks of tankers. J. Offshore Mech. Arctic Eng. 129, 48–55.
Guedes Soares, C., Garbatov, Y., 1998. In: Lydersen, S., Hansen, G.K., Sandtorv, H.A. (Eds.), Non-linear Time Dependent Model of Corrosion for the Reliability Assessment of Maintained Structural Components. Safety and Reliability, Balkema, Norway.
Guedes Soares, C., Garbatov, Y., Zayed, A., et al., 2005. Non-linear corrosion model for immersed steel plates accounting for environmental factors. Trans. - Soc. Nav. Archit. Mar. Eng. 111, 194–211.
Guedes Soares, C., Garbatov, Y., Zayed, A., et al., 2008. Corrosion wastage model for ship crude oil tanks. Corrosion Sci. 50 (11), 3095–3106.
IMO, 2010. Report of the Maritime Safety Committee on its Eighty-Seventh Session (MSC 87/26). Maritime Safety Committee. International Maritime Organization, London, UK.
IMO, 2015. International Goal-Based Ship Construction Standards for Bulk Carriers and Oil Tankers. International Maritime Organization,, London, UK.
Kim, H.C., 2010. Korea's Ship – Chapter 16: Design Life of Ship and Prospect of

Technology Development (by Korean Language). Jisungsa Publisher, Seoul, Korea.
Kim, D.K., Kim, S.J., Kim, H.B., et al., 2015. Ultimate strength performance of bulk carriers with various corrosion additions. Ships Offshore Struct. 10 (1), 59–78.
Kim, D.K., Kim, B.J., Seo, J.K., et al., 2014a. Time-dependent corrosion damage on the development of residual strength – grounding damage index diagram. Ocean Eng. 76, 163–171.
Kim, D.K., Kim, H.B., Zhang, X.M., et al., 2014b. Ultimate strength performance of tankers associated with industry corrosion addition practices. Int. J. Nav. Archit. Ocean Eng. 6 (3), 507–528.
Kim, D.K., Lim, H.L., Yu, S.Y., 2019a. Ultimate strength prediction of T-bar stiffened panel under longitudinal compression by data processing: A refined empirical formulation. Ocean Eng. 192, 106522.
Kim, D.K., Park, D.K., Kim, H.B., et al., 2012a. The necessity of applying the common corrosion addition rule to container ships in terms of ultimate longitudinal strength. Ocean Eng. 49, 43–55.
Kim, D.K., Park, D.K., Kim, J.H., et al., 2012b. Effect of corrosion on the ultimate strength of double hull oil tankers - Part I: stiffened panels. Struct. Eng. Mech. 42 (4), 507–530.
Kim, D.K., Park, D.K., Park, D.H., et al., 2012c. Effect of corrosion on the ultimate strength of double hull oil tankers - Part II: hull girders. Struct. Eng. Mech. 42 (4), 531–549.
Kim, D.K., Wong, E.W.C., Cho, N.K., 2020. An advanced technique to predict time-dependent corrosion damage of onshore, offshore, nearshore and ship structures: Part I = Generalisation. Int. J. Nav. Architect. Ocean Eng., IJNAOE_319. In press.
Kim, D.K., Wong, E.W.C., Lee, E.B., et al., 2019b. A method for empirical formulation of current profile. Ships Offshore Struct. 14 (2), 176–192.
Kim, D.K., Zalaya, M.A., Choi, H.S., et al., 2017. Safety assessment of corroded jacket platform considering decommissioning event. Int. J. Automot. Mech. Eng. 14 (3), 4462–4485.
Melchers, R.E., 2001. Probabilistic modelling of immersion corrosion of steels in marine waters. In: The 20th International Conference on Offshore Mechanics and Arctic Engineering Conference (OMAE 2001), 3-8 June, Rio de Janeiro, Brazil.
Melchers, R.E., 2003a. Mathematical modelling of the diffusion controlled phase in marine immersion corrosion of mild steel. Corrosion Sci. 45 (5), 923–940.
Melchers, R.E., 2003b. Modeling of marine immersion corrosion for mild and low alloy steels – Part 1: phenomenological model. Corrosion (NACE) 59 (4), 319–334.
Melchers, R.E., 2012. Modeling and prediction of long-term corrosion of steel in marine environments. Int. J. Offshore Polar Eng. 22, 257–263.
Melchers, R.E., Chaves, I.A., Jeffrey, R., 2016. A conceptual model for the interaction between carbon content and manganese sulphide inclusions in the short-term seawater corrosion of low carbon steel. Metals 6 (6), 1–13.
Mohd Hairil, M., Kim, D.K., Kim, D.W., et al., 2014a. A time-variant corrosion wastage model for subsea gas pipelines. Ships Offshore Struct. 9 (2), 161–176.
Mohd Hairil, M., Kim, D.W., Lee, B.J., et al., 2014b. On the burst strength capacity of an aging subsea gas pipeline. J. Offshore Mech. Arctic Eng. 136 (4), 1–7, 041402.
Mohd Hairil, M., Paik, J.K., 2013. Investigation of the corrosion progress characteristics of offshore subsea oil well tubes. Corrosion Sci. 67, 130–141.
Ozguc, O., 2020. Conversion of an oil tanker into FPSO in Gulf of Mexico: strength and fatigue assessment. Ships Offshore Struct. https://doi.org/10.1080/17445302.2020.1790298. In press.
Paik, J.K., Kim, D.K., 2012. Advanced method for the development of an empirical model to predict time-dependent corrosion wastage. Corrosion Sci. 63, 51–58.
Paik, J.K., Kim, D.K., Kim, M.S., 2009. Ultimate strength performance of Suezmax tanker structures: pre-CSR versus CSR designs. Int. J. Maritime Eng. 151 (Part A2), 39–58.
Paik, J.K., Lee, J.M., Hwang, J.S., et al., 2003a. A time-dependent corrosion wastage model for the structures of single- and double-hull tankers and FSOs and FPSOs. Mar. Technol. 40 (3), 201–217.
Paik, J.K., Melchers, R.E., 2008. Condition Assessment of Aged Structures. CRC Press, New York, USA.
Paik, J.K., Thayamballi, A.K., Park, Y.I., et al., 2004. A time-dependent corrosion wastage model for seawater ballast tank structures of ships. Corrosion Sci. 46 (2), 471–486.
Paik, J.K., Thayamballi, A.K., Park, Y.I., et al., 2003b. A time-dependent corrosion wastage model for bulk carrier structures. Int. J. Maritime Eng. 145 (A2), 61–87.
Petersen, R.B., Melchers, R.E., 2016. Model for the long-term corrosion of cast iron pipes buried in soil. In: The 5th International Symposium on Life-Cycle Engineering (IALCCE 2016), 16-19 October, Delft, The Netherlands.
Rahbar-Ranji, A., Niamir, N., Zarookian, A., 2015. Ultimate strength of stiffened plates with pitting corrosion. Int. J. Nav. Archit. Ocean Eng. 7 (3), 509–525.
Rajput, A., Park, J.H., Noh, S.H., et al., 2019. Fresh and sea water immersion corrosion testing on marine structural steel at low temperature. Ships Offshore Struct. https://doi.org/10.1080/17445302.2019.1664128. In press.
Ringsberg, J.W., Li, Z., Johnson, E., et al., 2018. Reduction in ultimate strength capacity of corroded ships involved in collision accidents. Ships Offshore Struct. 13 (Sub 1), 155–166.
Wang, Y, Downes, J., Wharton, J.A., et al., 2018. Assessing the performances of elastic-plastic buckling and shell-solid combination in finite element analysis on plated structures with and without idealised corrosion defects. Thin-Walled Struct. 127, 17–30.
Wang, R., Guo, H., Shenoi, R.A., 2020b. Experimental and numerical study of localized pitting effect on compressive behavior of tubular members. Mar. Struct. 72, 102784.
Wang, R., Guo, H., Shenoi, R.A., 2020a. Compressive strength of tubular members with localized pitting damage considering variation of corrosion features. Mar. Struct. 73, 102805.
Wong, E.W.C., Kim, D.K., 2018. A simplified method to predict fatigue damage of TTR subjected to shortterm VIV using artificial neural network. Advances in Engineering Software 126, 100–109.
Yamamoto, N., Ikegami, K., 1998. A study on the degradation of coating and corrosion of ship's hull based on the probabilistic approach. J. Offshore Mech. Arctic Eng. 120 (3), 121–128.
Yang, H.Q., Zhang, Q., Tu, S.S., et al., 2016. A study on time-variant corrosion model for immersed steel plate elements considering the effect of mechanical stress. Ocean Eng. 125, 134–146.